ANALYSIS OF THE PATTERNS OF DISTRIBUTION OF ZOOPLANKTON AGGREGATIONS FROM AN ACOUSTIC DOPPLER CURRENT PROFILER

PAUL E. SMITH
National Marine Fisheries Service
Southwest Fisheries Center
P.O. Box 271
La Jolla, California 92038

MARK D. OHMAN
Marine Life Research Group, A-027
Scripps Institution of Oceanography
University of California, San Diego
La Jolla, California 92093

LAURENCE E. EBER
National Marine Fisheries Service
Southwest Fisheries Center
P.O. Box 271
La Jolla, California 92038

ABSTRACT

A test set of data of volume reverberation, measured from the R/V New Horizon, nominally from 12–240-m depth in 4-m intervals, was taken in April 1988 using a 307-kHz acoustic Doppler current profiler (ADCP). A vertical profile was produced each minute for three days over the San Diego Trough off southern California. The results show kilometer-scale zooplankton aggregations with somewhat larger gaps between them. The area profiles had about 10% coverage of zooplankton aggregations. Aggregation target strengths were usually stronger during the morning and evening migrations. Migration rates were of the order of 5–8 cm s^{-1} during ascent and 3–4 cm s^{-1} during descent. Zooplankton aggregations were of horizontal dimensions intermediate between fish schools and groups of schools.

RESUMEN

En abril de 1988, a bordo del buque de investigación New Horizon, se colectó una serie de datos de volumen de reverberación, haciendo uso de un aparato de 307 kHz para perfilar la corriente doppler acústica (PCDA), abarcando una profundidad de 12 a 240 m en intervalos de 12 m. Se midió un perfil vertical cada 1 minuto, por un período de 3 días, en la Depresión de San Diego, frente al sur de California. Los resultados indican agregaciones de zooplancton en escalas de kilómetros, con espacios algo más grandes entre las mismas. Aproximadamente 10% del área de los perfiles presentaron agregaciones de zooplancton. Las fuerzas de blanco de agregaciones fueron, en general, más fuertes durante las migraciones matutinas y vespertinas. Las tasas de migración fueron del orden de los 5 a 8 cm seg^{-1} durante el ascenso y de los 3 a 4 cm seg^{-1} durante el descenso. Las dimensiones horizontales de las agregaciones de zooplankton fueron intermedias entre cardúmenes de peces y grupos de cardúmenes.

INTRODUCTION

Distributional patterns in the pelagic habitat are known to exist at several time and space scales (Haury et al. 1978; Greenlaw and Pearcy 1985). Some spatial scales have been evaluated for some planktivorous pelagic schooling fish (Graves 1977; Fiedler 1978; Smith 1978b), zooplankton (Star and Mullin 1981; Haury and Wiebe 1982; Pieper and Holliday 1984), and mesopelagic micronekton (Greenlaw and Pearcy 1985). Two aspects of plankton sampling that must take account of these scales are (1) estimation of the abundance of a species and (2) an understanding of the interactions between planktonic organisms and their immediate environment, principal predators, competitors, and food organisms.

Vertical and horizontal integration can increase the precision of estimates of abundance of "patchy" organisms in the plankton sample (Wiebe 1972). The integrated sample, however, may underestimate the local density of an organism by sampling volumes at inappropriate depths, or may include species with which the target species never interacts. Resolving the patchy dispersion of prey within a fluid volume is important for estimating attack rates by predators (Ohman 1988a).

The space scales relevant to a particular population or process are invisible in the pelagic habitat. Pilot sampling studies are necessary to help formulate and constrain the questions to be answered (Andrews and Mapstone 1987). Acoustic methods can be useful for such preliminary surveys, as a means to obtain rapid, broad coverage, and as a tool to direct other, invasive sampling methods. Acoustic methods are not generally useful for identifying organisms or precisely estimating their biomass. A continuous acoustic record can be used to delineate spatial scales that must be encompassed or resolved (Holliday 1985).

Studies of the scale and intensity of fish schools have been used to design and interpret surveys of northern anchovy eggs (Smith 1970; Hewitt et al. 1976; Graves 1977; Fiedler 1978; Smith 1978a,b, 1981; Smith and Hewitt 1985a,b). Two major find-

ings of this work that depended on acoustic technology are that (1) on the small scale, within a school, the biomass of fish is on the order of 15,000 grams per square meter of horizontal surface, and their consumption of plankton would be approximately 750 grams per square meter of fish school horizontal surface per day; and (2) the fish schools of tens of meters in diameter are assembled in concentrations of shoal groups extending for tens of kilometers. We do not know the rules of assembly of shoal groups: one mechanism could be that schools' swimming speeds decrease and turning behavior increases when the school is in the upper ranges of plankton biomass. The lower ranges of plankton biomass could be a temporary result of foraging groups of schooled fish (Koslow 1981).

In addition to the spatial complexity of the pelagic habitat at several horizontal scales, rapid changes in the vertical distribution of organisms at dawn and dusk are well known (Enright 1977; Pieper and Bargo 1980). The impact of these migrators on the distribution pattern of their prey must be added to the direct effects of diel vertical migration on the distribution of plankton. Initial time and space scale information from acoustical methods may be useful in designing the most effective direct sampling procedures for studies of fine-scale processes and of geographic-scale population abundance.

Acoustic profiles may be used to estimate the scale and intensity of patchiness and to help specify the number, size, and placement of samples. The primary sampling design questions to be asked in pelagic studies are:

How many samples are needed?
How big should the sample units be?
At what separation distance can adjacent sample units be said to be effectively independent?
Over what spatial and temporal scales are processes operating?
What are limits of the temporal and spatial scales to be used for such studies?

It is the purpose of this study to report the qualitative spatial analysis from several days of continuous acoustical sampling. From these records, we will summarize the incidence of biological aggregations, their spatial dimensions, the dimensions of the spaces between aggregations, the depth distribution of aggregations, and the rates of change in depth.

METHODS

The pilot study was conducted in a 5 by 15-n. mi. area oriented SE NW about 25 n. mi. west north-

west of San Diego (figure 1). The equipment used included a 307-kHz acoustic Doppler current profiler (ADCP)[1], a multiple opening-closing net, and environmental sensing system (MOCNESS, Wiebe et al. [1985]), and standard hydrographic bottle casts. It is important to note that the ADCP had not been calibrated in the amplitude domain and that the effect of methods of conditioning the amplitude signal have not been studied. The Sea-Bird Electronics temperature sensor on the MOCNESS frame was calibrated against deep-sea reversing thermometers. Chlorophyll a and pheopigments retained on Gelman GF/F filters were extracted in refrigerated acetone and analyzed on a Turner Designs Model 10 fluorometer. Dissolved oxygen was determined by the Carpenter (1965) modification of the Winkler titration method. The MOCNESS (20 nets, 1-m^2 effective mouth area, 333-μm mesh) was towed at about 50–75 cm s^{-1}. A nighttime profile was made from 500 m to the surface in approximately 50-m intervals between 0131 and 0401 on April 6, 1988. A comparable daytime profile was made from 1330 to 1510 on April 6. Volume filtered per haul averaged 354 m^3 (range 156–927 m^3). Samples were preserved in 10% Formalin buffered with sodium borate. Select copepod species were enumerated after subsampling with a Stempel pipette; when organisms were rare the entire sample was counted.

Acoustical Methods

The primary function of the ADCP is to sense current direction and speed as a function of depth. It accomplishes this by detecting the Doppler frequency shift of backscattered sound from planktonic organisms, particles, and small-scale discontinuities in the water column. This frequency shift is proportional to the relative velocity between the backscattering source and the transducer. The change in frequency is measured by four transducers. Unlike echo sounders having the transducer aimed downward, or sonars (sonically determined azimuth and range) having the transducer directed laterally at any angle with reference to the bow, the four ADCP transducers are oriented at 30° from the vertical: approximately forward, aft, right abeam, and left abeam (figure 2). This means that the axes of the complementary beams are as far apart as the depth (2 × sin (30°) = 1) below the transducer. In
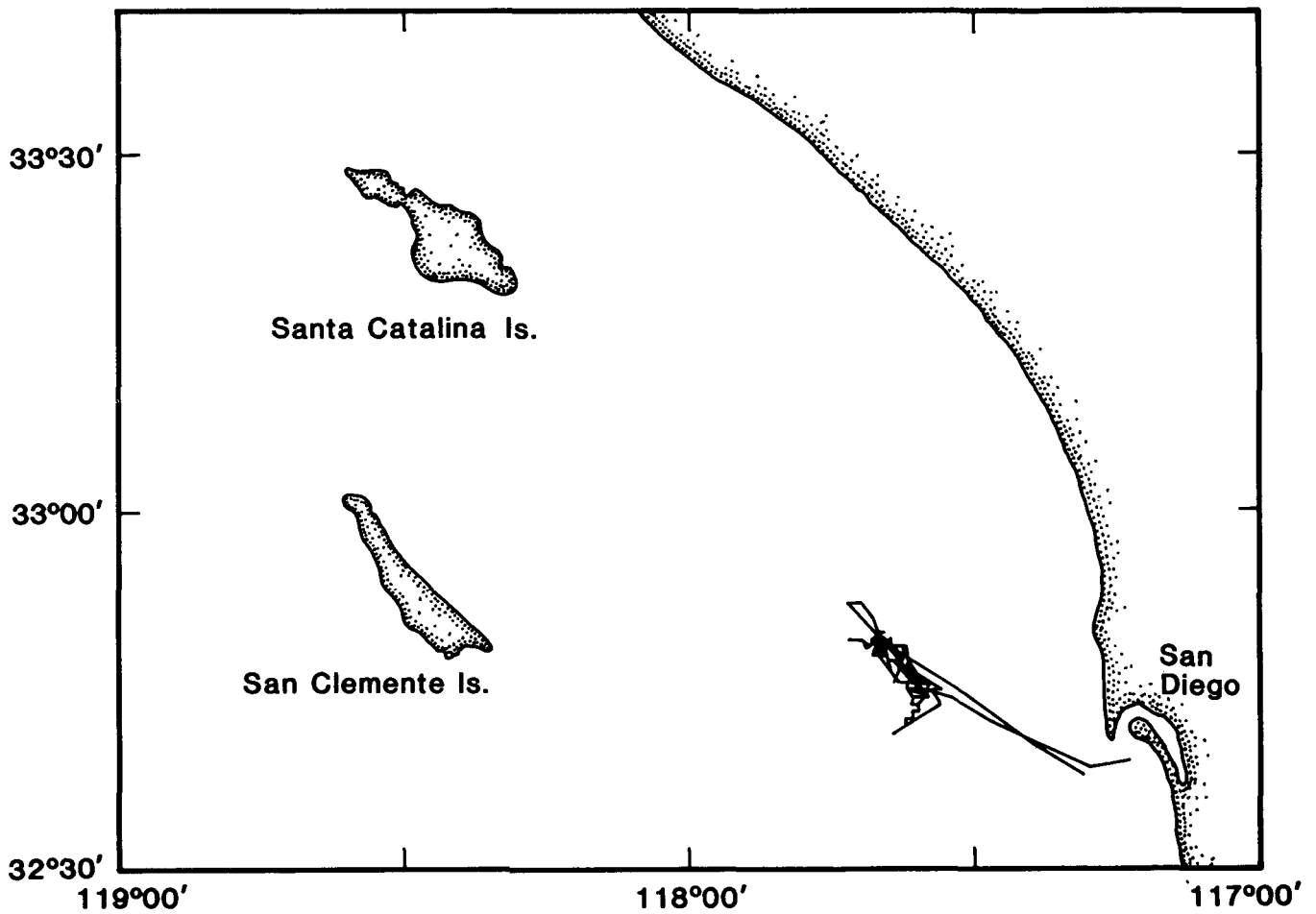
Figure 1.   Track of R/V *New Horizon* during ZB1 cruise. Data were collected during the entire cruise. See figure 8.

this report we analyze the information content of the echo amplitudes, rather than their frequencies.

The speed of sound in water is approximately 1500 meters per second. Therefore a sound oscillation of 300,000 cycles per second (Hz) has a wavelength of 5 mm; in general, insonified objects much larger than 5 mm scatter sound more efficiently than objects equal to or smaller than 5 mm (Holliday 1980). The proportion of the sound transmitted through, reflected from, and scattered around the object is influenced by small contrasts between the compressibility and density of water and these features of the object. For example, an organism with a bony skeleton, scaly integument, and air bladder returns much more sound than an organism which is primarily protoplasm. Similarly, organisms that are aggregated into patches or layers return more scattered sound per unit of local volume than the same organisms would if distributed evenly throughout a larger volume.

The probability that the acoustic pulse will encounter a target increases with depth because the widths of each acoustic beam increase with depth (figure 2). The probability of detection of a given target decreases with depth because the sensitivity of the receiver is fixed but the sound available for reflecting or scattering is decreasing as the inverse square of the range. In addition, there is a frequency-specific attenuation of sound in water, with more sound lost as a function of range in the higher frequencies. To use the ADCP as an acoustic sampling system, we must be able to define the conditions of encounter and the probability of detection. Targets smaller than 240 m cannot be resolved at the deepest depths because of the transducer beam geometry.

The ADCP used in the April cruise operated at 307.2 kHz. The transducer installation on the R/V *New Horizon* was 4 m deep (the draft of the ship), and the outgoing pulse was set at 4-m length (2.7
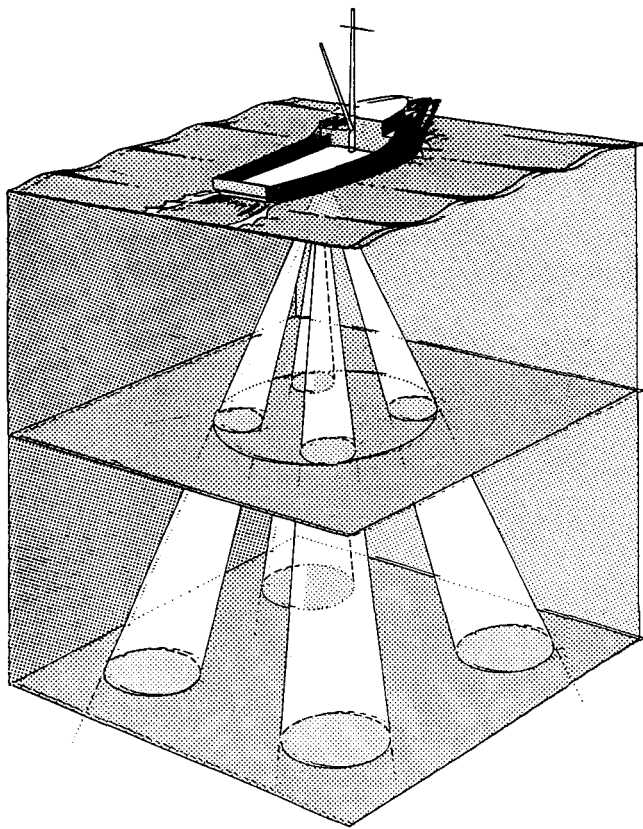
Figure 2. Diagram of the insonification pattern of an acoustic Doppler current profiler (RDI Inc. manual). Contrary to the diagram, the actual orientation of beams is 2 fore and aft and 2 left and right.

msec). Since the near-field return data (4 m) were not collected, the first data on the water column acoustic backscatter were obtained from a depth of about 12 m (figure 3). All graphical zero depths actually refer to 12 m. For each pulse, the amplitude of the return and the estimated velocity of the layer were stored in 60 depth "bins," each representing 4 m. Following nearly a minute of pulses at 1-second intervals, the ensemble average of each bin was calculated, and this average was stored as a compact binary record on a floppy disk. The ensemble averages of the previous profile were also displayed at the operator's console as the next ensemble was being taken (figure 3). Two of the four vertical profiles stored each minute are the velocities of the 4-m layers relative to ship's motion, as a function of depth. One of these profiles displays current speed at right angles to the ship's motion, and the other in the direction of the ship's motion.

There are two accessory profiles. One is the automatic gain control (AGC), which indicates echo amplitude with depth, and the second is the "percent good" value, which indicates the percentage of pings exceeding the signal-to-noise threshold. Note
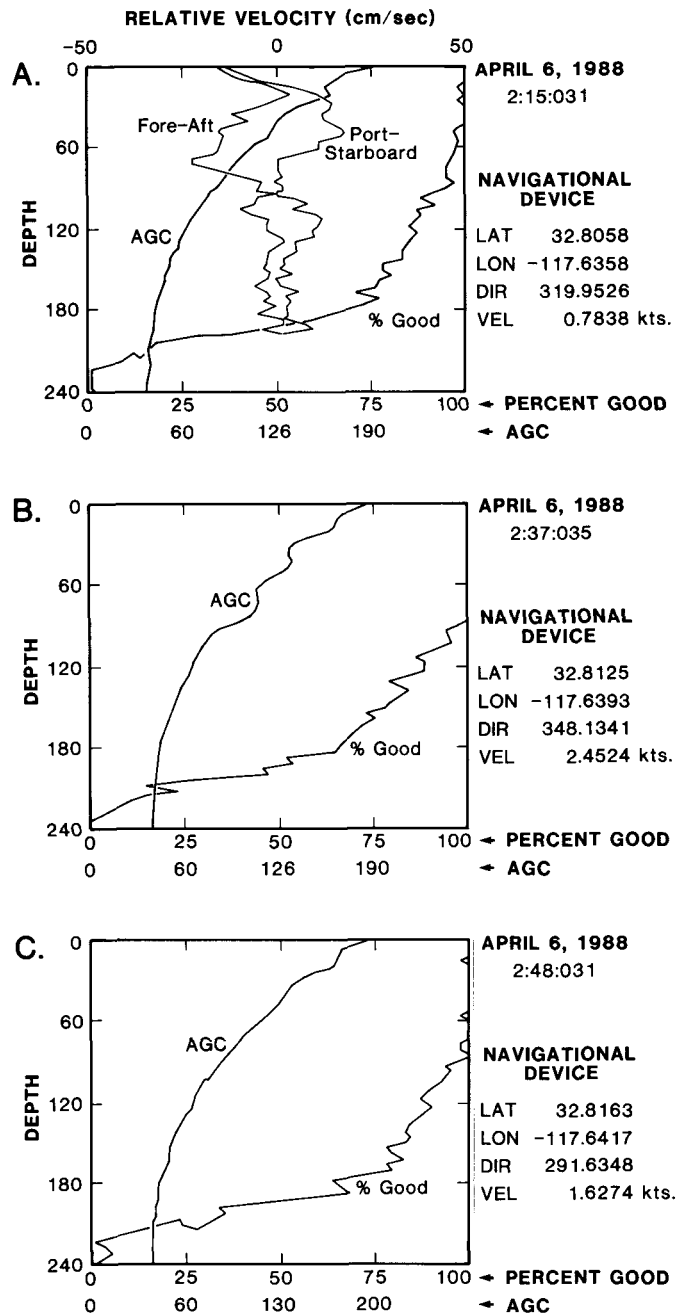

Figure 3. Specimen profiles. A, The velocity curves extend from 0 to 200 m and represent the water-layer motion after the effect of ship's motion in these planes has been removed. One velocity curve is the port-starboard velocity; the other is the fore-aft velocity. The curve labelled AGC is the automatic gain control. The last curve is the "percent good" value expressed as the percentage of pings in the ensemble that were analyzed for frequency at each 4-m depth interval. When this value drops below 25%, the analysis of velocities stops. B, Profile taken 22 minutes later, showing the effect of targets on the AGC profile. Velocity curves have been removed for clarity. C, Profile taken after the targets had passed.

in figure 3A that the AGC is primarily a decreasing function of depth and that "percent good" remains above 90% in the first 60 m below the ship, declines to 75% by 180 m, to 25% by 210 m, and to less than

Figure 4. A, Matrix of echo amplitude data direct from processor for 35 depth levels and 35 minutes, including the example profiles from figure 3. Analysis matrix from which this was extracted was 60 depth levels by 240 minutes. Top row is depth in meters. Bottom three rows are number of data points in matrix at depth, mean value of points, and standard deviation of values. B, Normalized data from A. The mean for each depth level was subtracted from each point at that depth level, and the difference was divided by the standard deviation. Original values are integers and means; standard deviations and normalized values are decimal numbers that have been truncated for display.

10% below 220 m. The profile in figure 3B was taken 22 minutes after 3A and is an example of the display of targets in the AGC curve at approximately 50 m and 80 m. The profile in figure 3C was made 11 minutes after 3B, when the ship had passed over the target displayed in figure 3B.

The decline in "percent good" profiles in the ensemble decreases the precision proportional to the square of the number of good profiles. This means that at some depth below the ship, there will be essentially no information on the pattern of zooplankton distribution. The depth at which this happens has not been determined, and all nonrandom pattern has been analyzed no matter at which depth it was detected in the 12- to 250-m range.

The compact binary record also includes temperature of the water at the transducer, time of day, course and speed of the ship, geographic position of the ship, and the settings of the ADCP console at the time the ensemble average was taken.

The original binary record was converted to ASCII code for analysis. Two text files were constructed in the laboratory from each original file created at sea. One file contains 4 hours of AGC echo-amplitude data, 240 1-minute ensemble averages at each of 60 4-m depth intervals (figure 4A). The other file contains the date/time group, latitude, and longitude for the ensemble at half-hour intervals. The mean and standard deviation of the 240 values at each depth were calculated. Within each depth, the mean was subtracted from the value, and the difference was then divided by the standard deviation (figure 4B). Each data set was smoothed by the weighting matrix (figure 5), which was selected to speed the contouring process and limit the number of contour segments stored (Eber 1987). Contours were drawn at the unit-positive values of 1 or above. For the purposes of this study, small positive and all negative values were discarded as noise or assumed to represent the positions of continuous rather than aggregated sources of backscattering. Schott and Johns (1987) also contoured anomalies of echo amplitude in a moored ADCP.

Data collected over the continental shelf were not used for interpreting the mean and standard deviation for normalizing. In general, the volume reverberation was elevated in waters shallower than 240 m. Thus in the first and last panels of figure 8, the depth-specific means and standard deviations were assembled from data profiles in which the bottom echo was excluded.

We attempted to use the global mean and standard deviation for the entire data set rather than use
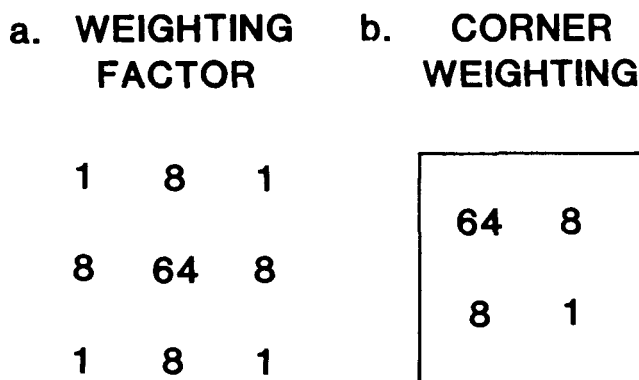
a. WEIGHTING FACTOR   **b. CORNER WEIGHTING**

Figure 5. Weighting matrices for the smoothing operator that were used to prepare the grid of values for contour tracking. a, The contoured value replaces the central value in the 9 contiguous bins and consists of a weight of 64 for the central value, 8 for each on-side contiguous value, and 1 for each diagonal contiguous value. B, At corners or edges the weighting matrix is adjusted to the location.

4-hour averages. The effect was to pool heterogeneous data, increase the standard deviation, and reduce the sensitivity of the normalized values to spatial structure. It is possible that electronics drift, long-term instrument instability, or environmentally induced changes in the signal amplitude make the derivation of a representative global mean and standard deviation uninterpretable with the present amount of data. To study these instrumental problems further, one must convert to calibrated sound sources and receiver sensitivities (Flagg and Smith 1989).

The ship's velocity was estimated from the file of dates, times, and geographic position. The sequential geographic positions nearest to each half hour were evaluated for distance traveled in the elapsed time. The difference in latitude in degrees was multiplied by 60 to obtain nautical miles, and by 1852 to obtain meters in that plane. The difference in longitude in degrees was multiplied by 60 and the cosine of the latitude (about 0.85 at the latitude of this study) to obtain nautical miles, and by 1852 to obtain meters. The distance in meters was calculated as the square root of the sum of squares of the latitudinal and longitudinal differences.

Aggregations were arbitrarily defined as those shapes within the 1 standard deviation-contour, which contained a contour of 2 or more standard deviations. Aggregations were assigned an aggregation serial number. We also determined the shallowest and deepest depths of each aggregation.

To estimate the horizontal extent, we measured the proportion of the aggregation's horizontal extent relative to the half-hour interval of distance traveled. The aggregation was then assigned a horizontal width in meters. For example, if the aggre-
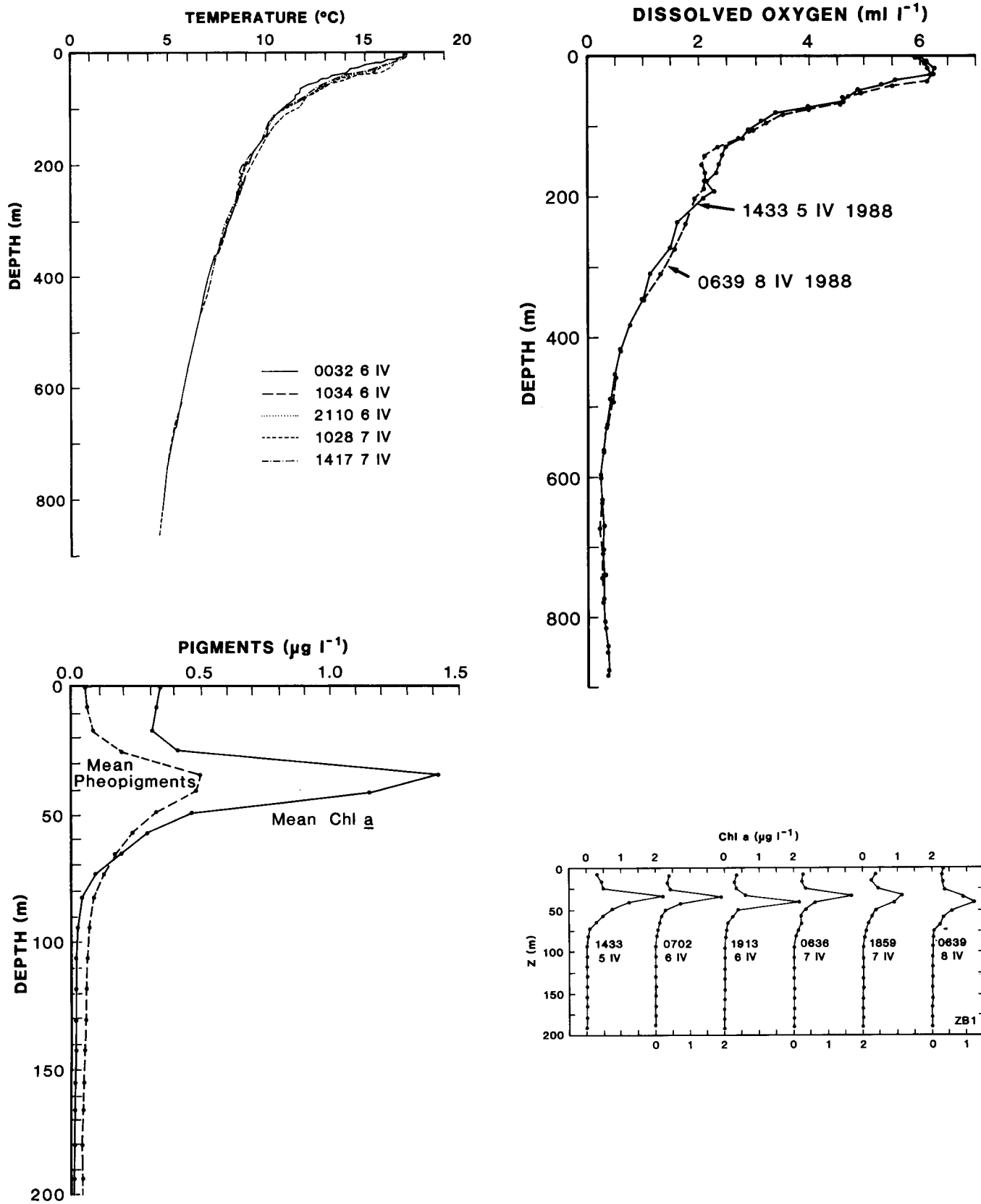
Figure 6. Vertical profiles: A, five temperature profiles; B, two dissolved oxygen profiles; C, means of six chlorophyll *a* and pheopigment profiles; D, six chlorophyll *a* profiles.

gation persisted for 10 minutes and the distance traveled in that half hour was 3200 m, the aggregation was said to extend 1070 m. The vertical plane area of each aggregation was estimated as the product of the vertical and horizontal dimensions. The sum of the vertical plane aggregation areas was estimated for each 4-hour period. The vertical plane area insonified was calculated by adding the ship's meters of progress in 8 half-hour intervals and multiplying by the depth of observation or 240 m. Comparison of the two values yielded an estimate of "coverage." Since there were no perfectly rectangular aggregations, the aggregation areas represent an overestimate varying from about 25% for inscribed circles to a factor of two or more for diagonally extended aggregations. Data exist for correcting this bias and for improving precision by more frequent evaluation of ship's speed.

RESULTS

Environmental Description

Vertical profiles of temperature, dissolved oxygen, and chlorophyll a can be characterized as exhibiting similarity in shapes and values among repetitions. Five temperature profiles taken between April 6 and 7 showed temperatures declining evenly, with some structure from 17°C at the surface to 5°C at 800 m (figure 6A). Deep oxygen profiles made near the beginning of the cruise (1433, April 5) and the end of the cruise (0639, April 8)

showed similar gradients, with a subsurface shallow maximum and a deep minimum at about 600 m (figure 6B). Vertical profiles of pheopigments showed maxima of about 0.5 $\mu g\ 1^{-1}$ at or near the depth of the chlorophyll maximum layer (figure 6C). Six chlorophyll casts had distinct subsurface maxima of 1-2 $\mu g\ 1^{-1}$ between 35 and 45 m (figure 6D).

Vertical distributions of adult females of three species of calanoid copepods illustrate different types of behavior that influence acoustic sampling methods (figure 7). Because all three species were relatively abundant and are known to store lipids (Ohman 1988b), they should have affected backscattering at 307 kHz. Calanus pacificus californicus Brodskii was nonmigratory, remaining in the upper 50 m within acoustic range day and night (figure 7A). If the finer-scale vertical distribution of this species were constant over time and distance, a C. pacificus californicus layer would influence the mean but not the standard deviation of echo amplitude. Eucalanus californicus Johnson was also nonmigratory, but remained between 200 and 400 m day and night (figure 7B). Slight shifts in vertical distribution of E. californicus of a few tens of meters would bring it into and out of acoustic range, primarily affecting the standard deviation of echo amplitude. Metridia pacifica Brodskii underwent a distinct vertical migration (figure 7C). A daytime population mode at 200-150 entered the upper 50 m at night. Such a pronounced shift in vertical distribution would influence both the amplitude mean and stan-
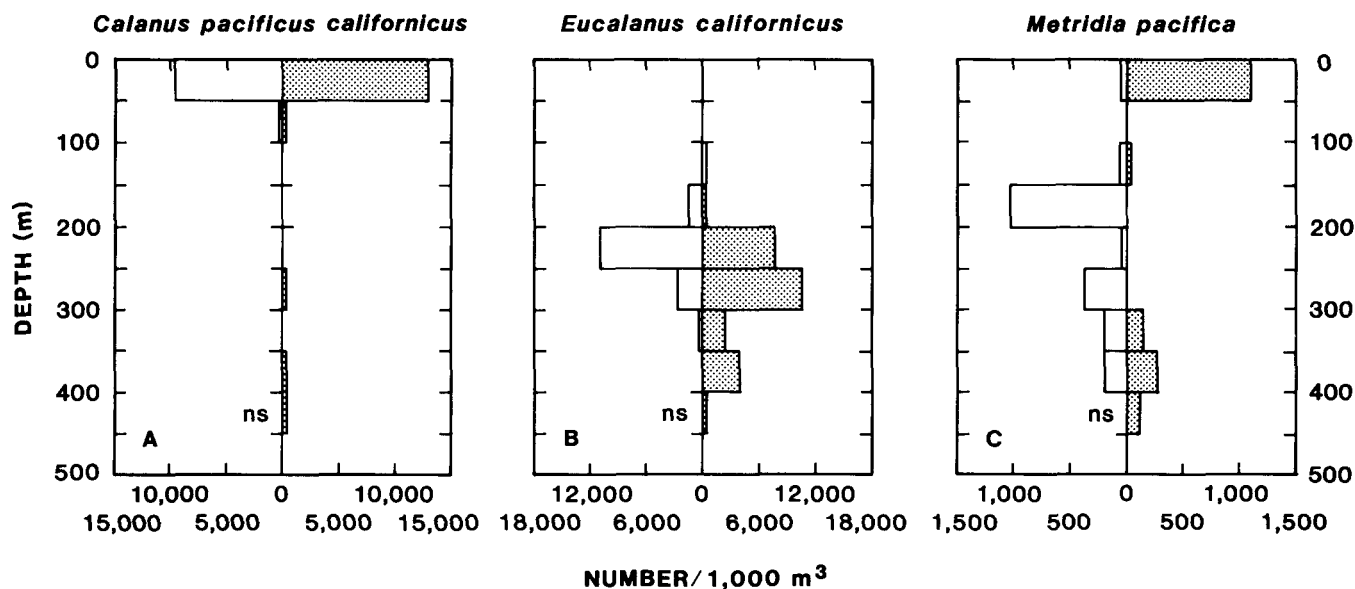

Figure 7. Day (open bars) and night (shaded bars) vertical distributions of adult females of the copepods Calanus pacificus californicus (A), Eucalanus californicus (B), and Metridia pacifica (C) on April 6, 1988. "ns" indicates that no sample was taken.

dard deviation. Note that a smaller segment of the *M. pacifica* population occurred at 400–300-m depth both day and night.

Euphasiid furciliae and adults, as well as other macrozooplankton taxa, also appeared in these samples.

General Appearance of Aggregations

There were no pronounced differences in the general appearance of aggregations between day and night. Both seem characterized by the appearance of shattered layers, shattered patches, and relatively smooth-edged patches. The physical size of the patches ranged from the threshold of detectabil-

ity to relatively large at all depths at all times of day. The largest and most coherent aggregations were detected during the vertical migrations at dawn and dusk (figure 8C, F, I, L, O, R).

Migration and Migration Rates

Coherent aggregations during the entire period of migration were observed in one of three dusk records and two of three dawn records. On the dawn of April 7 the descending layer bifurcated into distinct layers (figure 8L). Estimates of maximum ascent rate ranged from 5 to 8 cm s^{-1}, and estimates of the maximum descent rate ranged from 3 to 4 cm s^{-1}. Aggregation densities exceeded three standard
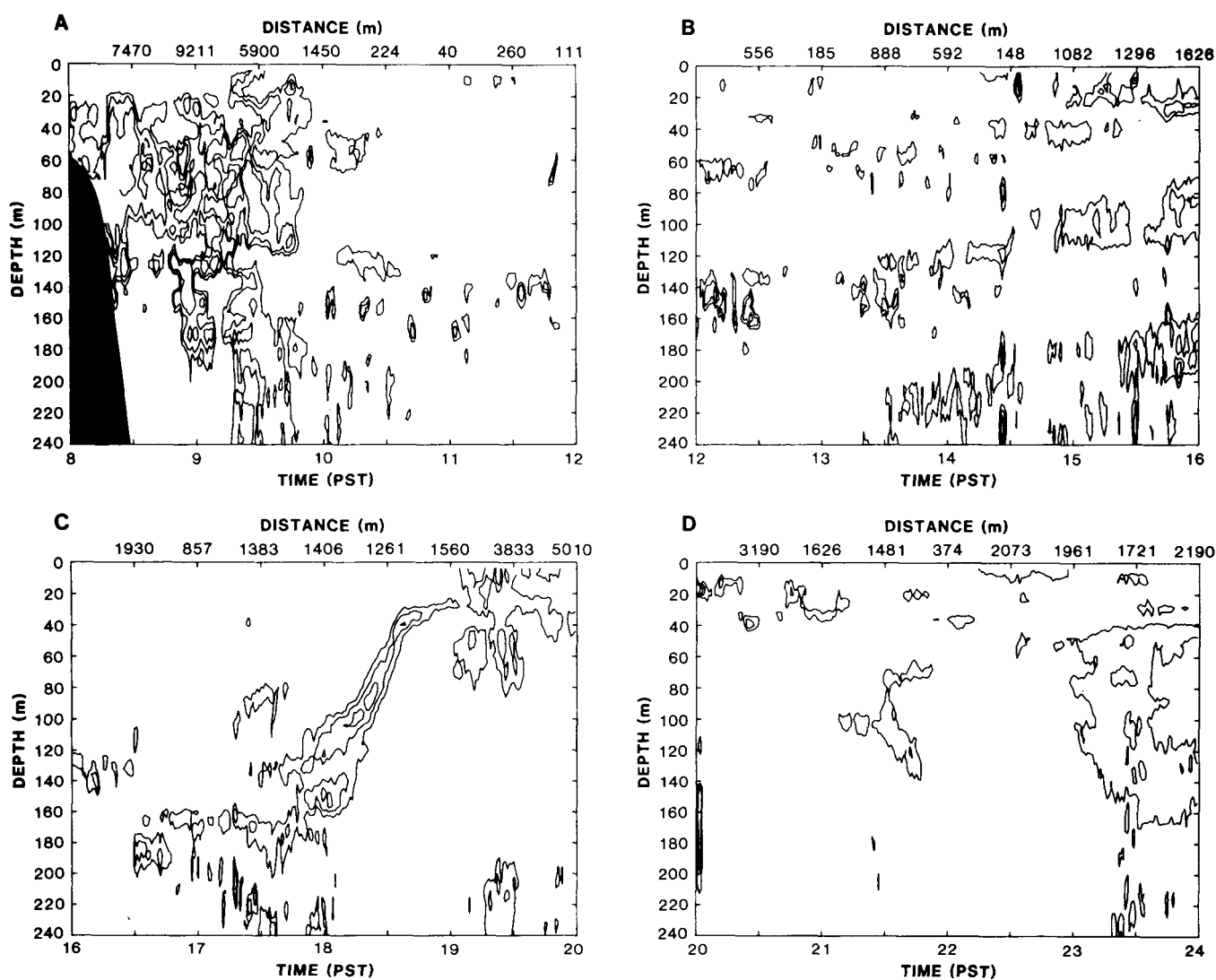

Figure 8 (continues on following three pages). A–S Each letter refers to a contoured data unit of 4 hours (less in 8S). The upper margin represents the straight-line distance between the ship's positions at the beginning and end of each half-hour interval. The figures are oriented on the page so that the day contours occupy the middle section, the dawn section for that calendar day is in the upper right, and the dusk section is in the lower left. The night contours are split between the upper left and the lower right. Contour interval is 1 standard deviation.
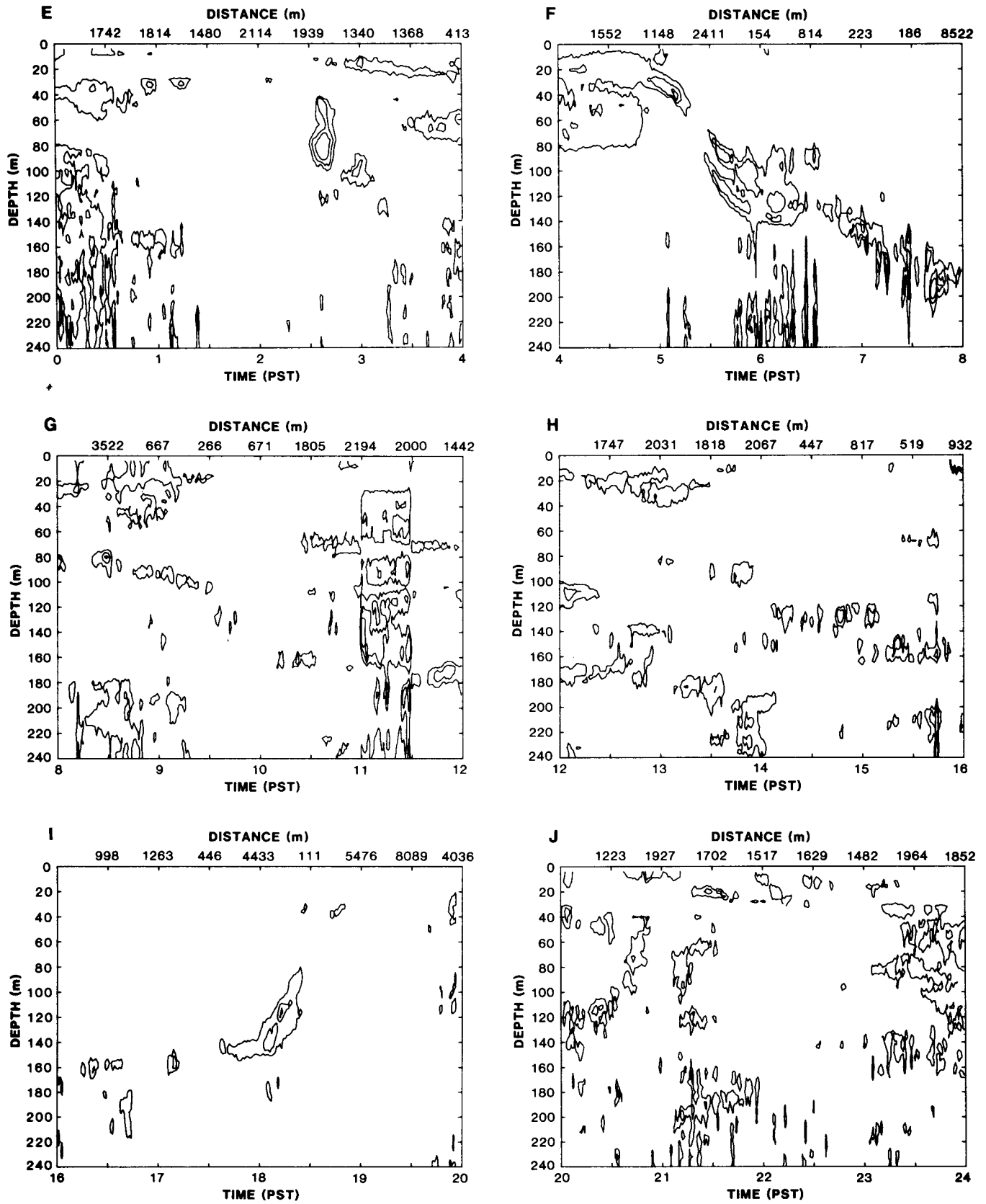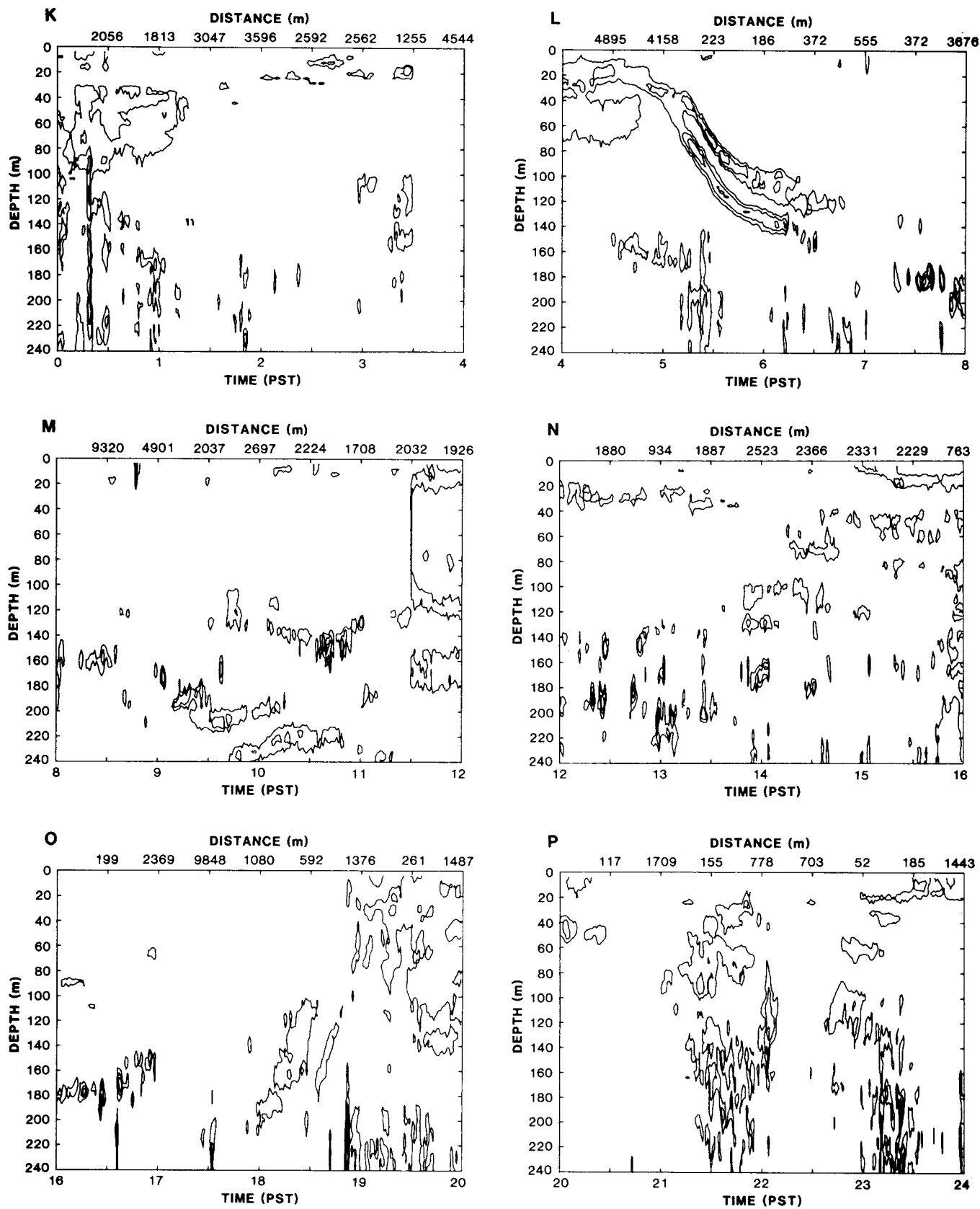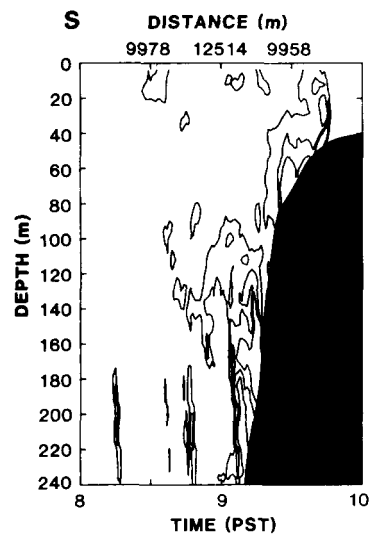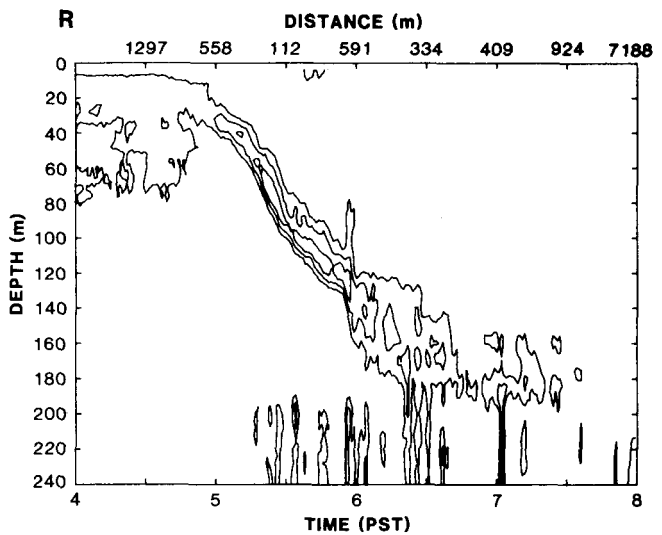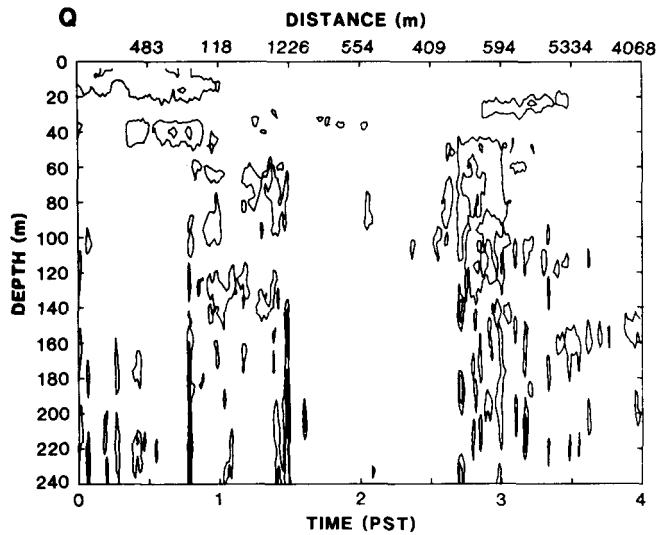
Figure 8 continued.

Figure 8 continued.

Figure 8 continued.

deviations above the mean in two of the three ascents and in all three descents.

Depth Distribution of Aggregations

Nearly twice as many of the 126 aggregations were detected at depth as near the surface (figure 9). The mean depth of aggregation is 134 m. At this stage of analysis it is not known if the cause of this distribution is simple or complex. The main cause of this imbalance is a surplus of aggregations at 180 m and 220 m and a deficiency of aggregations at 80 m and 100 m.

The simple explanation would be that this is the actual distribution of these aggregations. Complex explanations include (1) the width of the insonified volume increases at greater depths, increasing the chance of contact with patches; (2) some migrations from depth have destinations near the surface,

where the ADCP process does not insonify; (3) the fore-and-aft dimension of the insonified volume at depth detects aggregations that have been insonified many times during each ensemble average in the lower level but that are missed by insonifying the gaps among patches during their residence in the upper level; (4) the general level of reverberation in the upper level is higher, and the use of normalized detection is less effective there than in the lower level, where the aggregations stand out against a lower reverberation background level; and (5) the aggregation behavior of the organisms leads to compact aggregations at depth but more diffuse and less-detectable aggregations at the surface. The small value at 240 m may reflect the approach of the absolute depth for detection of aggregations from the surface with 307-kHz sound. At depths over 150 m there may be undetected aggregations owing to decreased signal-to-noise ratios.

Vertical Dimensions of Aggregations

More than half of the aggregations are less than 50 m in vertical dimension (figure 10). The mean vertical dimension of the aggregations was 54 m.
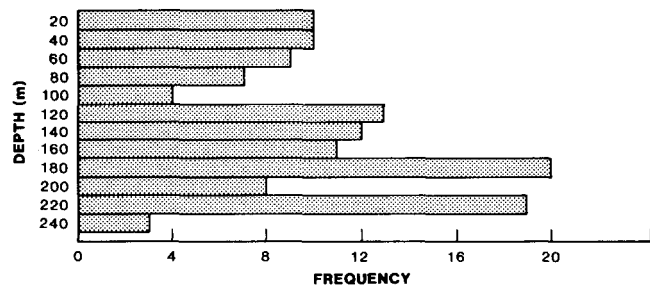

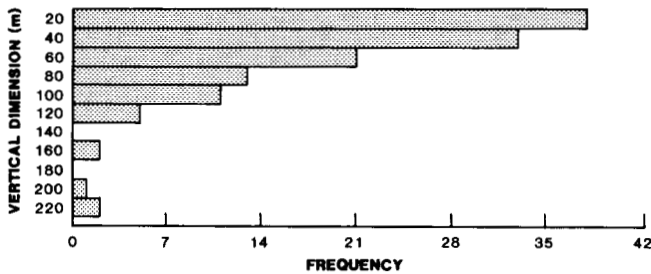Figure 9. The depth distribution of aggregations.

Figure 10. The vertical dimensions of aggregations.

Nearly 10% of the aggregations are more than 110 m in vertical extent. There has been no provision for excluding or estimating the incidence of aggregations that contact the upper or lower margin of the insonified volume; it appears unnecessary given the distribution of depths recorded here.

Horizontal Dimensions of Aggregations

The median horizontal dimension of aggregation is less than 750 m in the survey, and about 10% of the aggregations exceed 2250 m (figure 11). The arithmetic mean of the horizontal dimensions is 1268 m; the geometric mean is 519 m. This distribution is suitably approximated as a log normal distribution with parameters 6.251 and 1.440 (mean and standard deviation of ln values). The lower limit of detection of horizontal dimension is determined by ship's speed; at two knots (1 m s^{-1}) the lower limit would be 60 m; at 10 knots the lower limit would be 300 m. Much of this cruise involved the towing of plankton nets, and there was very little full-speed running between stations. Therefore the mode at horizontal dimensions less than 250 m may not be characteristic of cruise tracks at the higher speeds needed to cover wider geographic areas.

Horizontal Dimensions of Gaps between Aggregations

The median dimension of gaps between patches is less than 1500 m (figure 12). The arithmetic mean
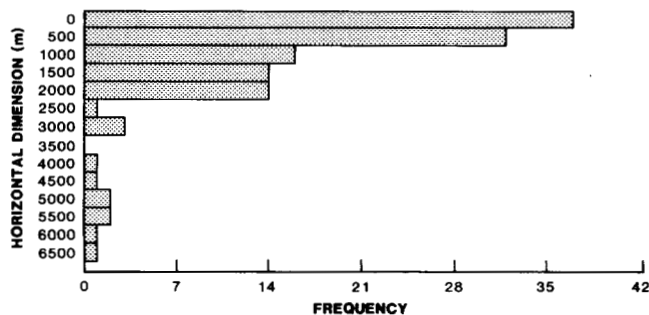

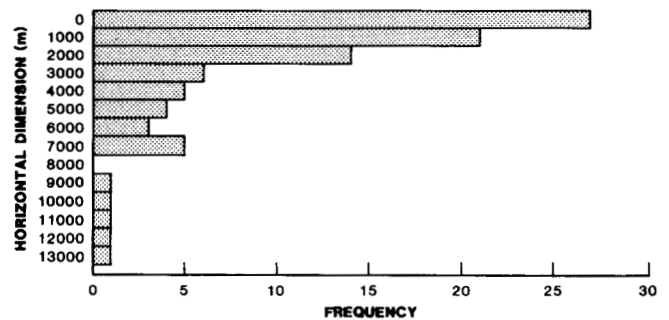Figure 11. The horizontal dimensions of aggregations.

Figure 12. The horizontal dimensions of gaps between aggregations.

of gap is 2553 m; the geometric mean is 1120 m. The distribution is approximately log normal, with parameters 7.021 and 1.428. About 10% of the gaps are longer than 6500 m. Horizontal dimensions of gaps among patches appear to be about double the horizontal dimensions of the patches.

Coverage

There is a clear mode in the coverage statistic at 10% (figure 13). Two-thirds of the 19 observations occurred in this interval. Two of the 19 4-hour segments were more than 25% covered with aggregations as defined.

Continental Shelf and Slope

Plankton aggregations over the continental shelf, slope, and shelf-break area appeared in both crossings of that region. Since both passages occurred in daylight, this area may represent a special case for shallow daytime plankton aggregations. The points of contact of these aggregations and the bottom may be of considerable importance to the demersal organisms in those depth zones.

Summary

Some important features of aggregations have been described with a sample of 126 aggregations measured in 19 4-hour segments. Limited data indicate that there are important plankton aggregations at the break between the continental shelf and slope. The vertical section of the aggregations covers approximately 10% of the water column in the upper 240 m. The mean thickness of aggregation is
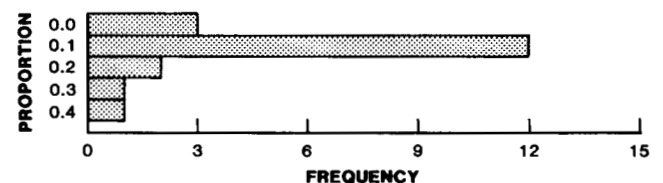

Figure 13. The distribution of proportion covered.

54 m, and about half of the aggregations are less than 50 m in vertical dimension. The mean horizontal dimension is 1268 m, and about half are less than 750 m across. In the horizontal plane, the gaps between aggregations are about twice as large as the aggregations. Vertical migration of the aggregations can usually be detected at dawn and dusk, but it is possible to be between aggregations at the time of migration in this locality.

DISCUSSION

The primary results of this study are that a procedure for estimating the structure of plankton aggregations has been defined, and some preliminary data have been gathered in one habitat near the southern California coast over the San Diego Trough. Depth distributions, vertical and horizontal dimensions of the aggregations, and gaps between aggregations are relatively consistent. Although the number of sections is small, it is possible to estimate the coverage of the vertical section over this coastal area as about 10%. Some of the strongest and most clearly defined aggregations were detected at the time of vertical migration at dawn and dusk.

The 307-kHz sound used for this study is probably capable of detecting aggregations of larger copepods (Castile 1975), euphausiids, the gas bubble of physonect siphonophores, and mesopelagic fishes. The migration rates of the aggregations detected on this cruise are in the upper range for migrating copepods. Enright (1977) estimated migration rates of 1 to 5 cm s^{-1} for the calanoid copepod Metridia pacifica from sequential net tows taken near the present study site. In laboratory respirometer chambers the euphausiid Euphausia pacifica has been clocked at up to 9.7 cm s^{-1} (Torres and Childress 1983).

Several works have emphasized the interactions between the pelagic layers and the ocean bottom at the continental shelf, shelf-break, and slope (Isaacs and Schwartzlose 1965; Genin et al. 1988; Holliday 1987; and Pieper et al., in press). In the brief transects of the continental shelf and slope (figures 8A and 8S) in this paper, it would appear that this "enriched" region is worthy of more study. It is likely to be a region of high productivity of demersal fishes that depend on food advected in pelagic layers and the migrations of some of the biota.

Although the technique used for estimating the size of patches is fundamentally different from that used by Greenlaw and Pearcy (1985), the gross appearance and vertical and horizontal dimensions of the patches are similar. The Greenlaw and Pearcy study was conducted with a single transducer and a fully calibrated system in the amplitude domain. Therefore the patches could be defined in absolute acoustic units by measuring contours at 5-dB intervals. From formal spatial spectral analysis, Greenlaw and Pearcy concluded that the vertical dimensions were of the order of tens of meters, and horizontal dimensions were km-scale. Our conclusions were based on statistical manipulation of unquantified amplitude domain acoustic signals, which appeared to be stable for short periods (4 hours). Our spatial scales were determined by direct measurement of arbitrary contour drawings, with contours placed at 1-standard-deviation intervals. In most of the drawings for this paper, this would involve 2–3-dB spacing for contours.

The horizontal dimension of plankton aggregations and of gaps between aggregations may be compared to fish schools, primarily the omnivorous planktivore northern anchovy (Engraulis mordax). In figure 14 are plotted the cumulative distributions of patch and gap dimensions from this study, a distribution of fish school sizes (Smith 1981), and the distribution of fish school group sizes (Fiedler 1978). Also, Star and Mullin (1981) described critical length scales for distributions of copepod stages and species, and found kilometer-scale aggregations to be the rule at a depth of 35 m. The slopes of the cumulative curves are lower for the patches and gaps than for the schools and school groups: one may infer from this that nekton spatial structures are under more behavioral control than the plankton aggregations.

It is clear from the size and intensity of the planktonic structures that considerable invasive sampling, with precise vertical and horizontal control of nets or pumps, will be necessary for studying the dynamics and interactions of these populations. The tactical deployment of such samplers directed by integrative acoustic devices like the ADCP will materially aid in understanding the primary interactions among schools and school groups of planktivorous fishes. In particular, the joint use of ADCP and directed sampling devices will be needed to model the foraging strategy of schooling fishes, and their search for, and effect on, the plankton aggregations to explain the relationship among spatial scales of primary production, secondary production, and the production of fishes.
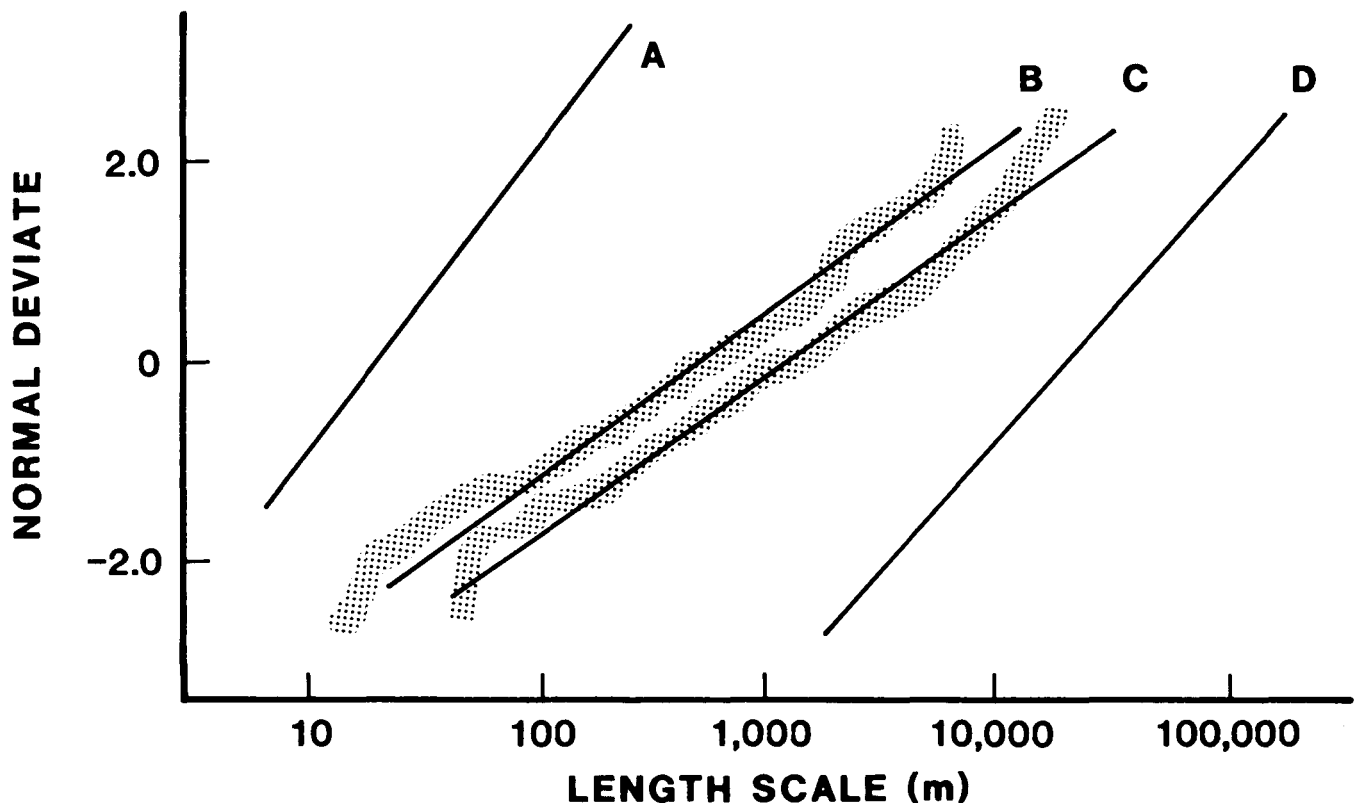
Figure 14. Comparison of the cumulative frequency distribution of horizontal dimensions of (A) fish schools (Smith 1981); (B) plankton aggregations; (C) gaps between plankton aggregations; and (D) fish shoal groups (Fiedler 1978). In curves B and C, a straight line has been fitted to the experimental data, which is represented with shading.

chlorophyll samples. Support came from the UC Ship Funds Committee and grant RM 252-S (to MDO) from the UCSD Academic Senate. We appreciate the assistance of Andrea Calabrese in data processing and data management. We also thank Ken Raymond and Roy Allen for drafting the figures and James Wilkinson for his help. Loren Haury and D. Van Holliday read the manuscript. Three reviewers also helped improve this manuscript.

LITERATURE CITED

Andrews, N. L., and B. D. Mapstone. 1987. Sampling and description of spatial pattern in marine ecology. In Oceanography and marine biology annual review, M. Barnes, ed. Aberdeen University Press, pp. 39–90.

Carpenter, J. H. 1965. The Chesapeake Bay Institute technique for the Winkler dissolved oxygen method. Limnol. Oceanogr. 10:141–143.

Castile, B. D. 1975. Reverberation from plankton at 330 kHz in the western Pacific. J. Acoust. Soc. Am. 58:972–976.

Eber, L. E., 1987. Environmental data mapping program — EDMAP. NOAA/NMFS Southwest Fisheries Center Admin. Rept. LJ–87–25.

Enright, J. T. 1977. Copepods in a hurry: sustained high-speed upward migration. Limnol. Oceanogr. 22:118–125.

Fiedler, P. C. 1978. The precision of simulated transect surveys of northern anchovy, Engraulis mordax, school groups. Fish. Bull. U.S. 76:679–685.

Flagg, C. N., and S. L. Smith. 1989. On the use of the acoustic Doppler current profiler to measure zooplankton abundance. Deep-Sea Res. 36(3A):455–474.

Genin, A., L. Haury, and P. Greenblatt. 1988. Interactions of migrating zooplankton with shallow topography: predation by rockfishes and intensification of patchiness. Deep-Sea Res. 35:151–175.

Graves, J. 1977. Photographic method for measuring spacing and density within pelagic fish schools at sea. Fish. Bull. U. S. 75:230–234.

Greenlaw, C. F., and W. G. Pearcy. 1985. Acoustical patchiness of mesopelagic micronekton. J. Mar. Res. 43:163–178.

Haury, L. R., and P. H. Wiebe. 1982. Fine-scale multi-species aggregations of oceanic zooplankton. Deep-Sea Res. 29:915–921.

Haury, L. R., J. A. McGowan, and P. H. Wiebe. 1978. Patterns and process in the time-space scales of plankton distributions. In Spatial pattern in plankton communities, J. H. Steele, ed. New York: Plenum Press. Pp. 277–327.

Hewitt, R. P., P. E. Smith, and J. Brown. 1976. Development and use of sonar mapping for pelagic stock assessment in the California Current area. Fish. Bull. U.S. 74:281–300.

Holliday, D. V. 1980. Use of acoustic frequency diversity for marine biological measurements. In Advanced concepts in ocean measurements for marine biology, F. P. Diemer, F. J. Vernberg, and D. Z. Mirkes, eds. Belle W. Baruch Library in Marine Sciences No. 10. University of South Carolina Press.

———. 1985. Active acoustic characteristics of nekton. In Workshop on the biology and target acoustics of marine life, J. W. Foerster, ed. Dept. of Oceanography, U.S. Naval Academy Report.

———. 1987. Acoustic determination of suspended particle size spectra. "Coastal Sediments '87" WW Div./ASCE, New Orleans, La., May 12–14, 1987.

Isaacs, J. D., and R. A. Schwartzlose. 1965. Migrant sound scatterers: interaction with the sea floor. Science 150 (3705):1810–1813.

Koslow, J. A. 1981. Feeding selectivity of schools of northern anchovy, *Engraulis mordax*, in the Southern California Bight. Fish. Bull. U. S. 79:131–142.

Ohman, M. D. 1988a. Behavioral responses of zooplankton to predation. Bull. Mar. Sci. 43:530–550.

———. 1988b. Sources of variability in measurements of copepod lipids and gut fluorescence in the California Current coastal zone. Mar. Ecol. Progr. Ser. 42:143–153.

Pieper, R. E., and B. G. Bargo. 1980. Acoustic measurements of a migrating layer of the Mexican lampfish, *Triphoturus mexicanus*, at 102 kilohertz. Fish. Bull. U. S. 77:935–942.

Pieper, R. E., and D. V. Holliday. 1984. Acoustic measurements of zooplankton distributions in the sea. J. Cons. Int. Explor. Mer 41:226–238.

Pieper, R. E., D. V. Holliday, and G. S. Kleppel. In press. Quantitative zooplankton distributions from multifrequency acoustics. J. Plankton Res.

Schott, F., and W. Johns. 1987. Half-year-long measurements with a buoy-mounted acoustic Doppler current profiler in the Somali Current. J. Geophys. Res. 92:5169–5176.

Smith, P. E. 1970. The horizontal dimensions and abundance of fish schools in the upper mixed layer as measured by sonar. *In* Proc. of an int. symp. on biol. sound scattering in the ocean, G. B. Farquarhar, ed. Maury Center Report 805, Dept. of Navy.

———. 1978a. Biological effects of ocean variability: time and space scales of biological response. Rapp. P. V. Reun. Cons. Int. Explor. Mer 173:117–127.

———. 1978b. Precision of sonar mapping for pelagic fish assessment in the California Current. J. Cons. Int. Explor. Mer 38:31–38.

———. 1981. Fisheries on coastal pelagic schooling fish. *In* Marine fish larvae: morphology, ecology, and relation to fisheries, R. Lasker, ed. Washinton Sea Grant Program, Seattle.

Smith, P. E., and R. P. Hewitt. 1985a. Sea survey design and analysis for an egg production method of northern anchovy biomass assessment. *In* An egg production method for estimating spawning biomass of pelagic fish: application to the northern anchovy (*Engraulis mordax*), R. Lasker, ed. NOAA Tech. Rep. NMFS 36:17–26.

———. 1985b. Anchovy egg dispersal and mortality as inferred from close-interval observations. Calif. Coop. Oceanic Fish. Invest. Rep. 26:97–112.

Star, J. L., and M. M. Mullin. 1981. Zooplanktonic assemblages in three areas of the North Pacific as revealed by continuous horizontal transects. Deep-Sea Res. 28:1303–1322.

Torres, J. J., and J. J. Childress. 1983. Relationship of oxygen consumption to swimming speed in *Euphausia pacifica*. 1. Effects of temperature and pressure. Mar. Biol. 74:79–86.

Wiebe, 1972. A field invetigation of the relationship between length of tow, size of net and sampling error. J. Cons. Perm. Int. Explor. Mer 34:268–275.

Wiebe, P. H., A. W. Morton, A. M. Bradley, R. H. Backus, J. E. Craddock, V. Barber, T. J. Cowles, and G. R. Flierl. 1985. New developments in the MOCNESS, an apparatus for sampling zooplankton and micronekton. Mar. Biol. 87:313–323.